

# Data-Driven Modeling of a CO<sub>2</sub> Refrigeration System\*

Glenn Andreasen<sup>1</sup>, Jakob Stoustrup<sup>1</sup>, Roozbeh Izadi-Zamanabadi<sup>2</sup>, Ángel Á. Pardiñas<sup>3</sup>, Armin Hafner<sup>3</sup>

**Abstract**—This paper describes a data-driven method for system identification of a CO<sub>2</sub> refrigeration system. Traditionally, the interaction between the measured variables is not utilized as they are highly dependent on the refrigeration system. In this work a data-driven method, namely subspace identification, is investigated for deriving a control-oriented model such that the dynamic interaction in the refrigeration systems can be utilized for e.g. fault detection and diagnosis. The subspace identification is applied on laboratory data obtained from a test setup located at NTNU in Trondheim, Norway. The obtained results offer promising perspectives for performance improvement in fault detection and diagnosis methods as well as control strategies.

## I. INTRODUCTION

Refrigeration systems are widely used in the industry for cooling of goods. The physical configuration of these systems varies and depends on the required cooling capacity and operating conditions. In some cases, heat recovery and/or air conditioning (AC) units can also be included in a refrigeration system. Furthermore, to increase efficiency of the refrigeration systems, which use CO<sub>2</sub> as coolant, ejectors in a setup with intermediate compression may be utilized. Additionally, the dynamic/static characteristics of the used components (such as valves, compressors, condenser, etc.) depends on the provider and is not normally known in advance. [1]

For these reasons and the fact that refrigeration systems also exhibit nonlinear behaviors, design of controllers for these systems is a challenging task. These controllers are often based on first principle models and afterwards tuned by service people during the commissioning/retrofit phase. A more appealing approach would be to utilize a data-driven technique for controller designs. Likewise, data-driven techniques would be preferable for optimization purposes, fault detection and diagnosis (FDD) and fault tolerant control (FTC) [1], [2].

This work is focused on obtaining an off-line data-driven model (henceforth referred to as data-driven model) of a CO<sub>2</sub> refrigeration system with booster configuration (described in Sec. II) that can be utilized for control-oriented design purposes. The aim for the data-driven model is to capture the dynamics from input (associated actuator) to output (associated controlled variable) by use of the available

measurements. The resulting data-driven model is to be linear such that it is applicable for already known and well-defined control, optimization, FDD and FTC algorithms.

Over the past 50 years several papers on system identification have been published. Two of them [3], [4] resulted in numerous techniques, which are now covered by the label PEM (Prediction Error Method). These are based on optimization in least squares type criteria which have to be solved iteratively. The PEM techniques are well defined for linear SISO (Single Input Single Output) systems, however MIMO (Multiple Inputs Multiple Output) and non-linear systems are not covered to the same extent. Later on in the 1980, subspace identification techniques were introduced and since then several papers have been published as well as some books (see references [5], [6], [7] and references within). A drawback with utilizing PEM for MIMO system identification is that they are solved iteratively and are based on a (non-convex) optimization function, which suffer the risk of being stuck in a local minimum. Subspace techniques does not suffer from this risk [5].

In recent years, subspace techniques for process monitoring purposes have received increased attention [8], [9]. In the refrigeration system application field the authors in [2] have utilized a subspace system identification technique to generate a model that is used to design a model predictive control strategy.

Even though several papers (some mentioned previously) utilize data-driven approaches for various applications on different systems, there is still a large interest for further research on usage of data-driven techniques on complex industrial non-linear MIMO systems. This is mainly caused by the potential from the (increasingly) available I/O data and computational power. [10]

Application of the methods described above to refrigeration systems has only been pursued to a very limited extent and even less for systems that utilizes CO<sub>2</sub> as coolant. CO<sub>2</sub> as a coolant is increasingly utilized because of its reduced impact on the environment [11].

In section II the test setup is described. Section III describes the subspace identification method and section IV deals with the selection of the inputs used for the system identification. Section V evaluates the validation of the data-driven model and lastly, section VI presents the main conclusions of this work.

## II. CO<sub>2</sub> REFRIGERATION SYSTEM

A CO<sub>2</sub> refrigeration system located at NTNU/SINTEF laboratory is available. This system has been thoroughly described in [12] with sizing, components and possible

\*This work is supported by the Innovationsfonden, 7038-00100B, Denmark.

<sup>1</sup>Faculty of Electrical Engineering, Automation and Control, Aalborg University, 9220 Aalborg, Denmark ga, jakob@es.aau.dk

<sup>2</sup>Danfoss A/S, Denmark Roozbeh@danfoss.com

<sup>3</sup>Department of Energy and Process Engineering, NTNU, Trondheim, 7491, Norway angel.a.pardinas, armin.hafner@ntnu.no.com

configurations. Thus, only a brief overview of the relevant aspects of the system and the selected configuration is given here. In this work the system is set to booster configuration with refrigeration at medium temperature (MT), low temperature (LT), and air conditioning (AC), where the maximum loads are 60 kW, 13 kW, and 45 kW respectively. This configuration is selected for simplicity reasons. Fig. 1 illustrates a simplified schematic of the CO<sub>2</sub> refrigeration system with the mentioned configuration and the relevant and available measurements, where the measured values i.e. pressure, temperature, valve opening degree and load are denoted with P, T, OD and Q respectively. Redundant components (from a control-oriented perspective) are omitted from the schematic. Additionally, the heat recovery and gas cooler (GC) are represented by only one heat exchanger as heat recovery is not considered in this paper. The CO<sub>2</sub> system has a secondary side where all heat exchangers (LT, MT, AC, GC, desuperheater) are connected to either a mixture of glycol and water (henceforth referred to as glycol) or water. On the secondary side it is possible to control the load and outlet temperature of the glycol of each heat exchanger, thereby emulating consumer demand (e.g. food for MT and LT). The reader is referred to [12] for further details on the secondary side. For this configuration three parallel MT display cases are utilized where each display case is represented with a heat exchanger and an electronic expansion valve. The LT consist of a single display case and is designed in a similar manner. For each display case (both LT and MT) load, temperature and opening degree of the expansion valves are measured.

The controlled variables on the CO<sub>2</sub> side are itemized here:

- Pressure before the high pressure valve (HPV) is controlled with the HPV controller (type CCMT16 Danfoss valve).
- Temperature before the HPV is controlled with the three way valve. Both the temperature and the pressure (mentioned in the prior bullet) are controlled to reach a desired sub-cooling/trans-critical point.
- Pressure in the receiver is controlled with the bypass valve (BPV) of type CCMT42 Danfoss valve. Controlling this pressure reduces fluctuation in the coolant flow to the MT and LT cabinets.
- Superheat out of each display case (both MT and LT) are controlled with the individual expansion valve of type AKVH10 Danfoss (note in Fig. 1 the controllers are only illustrated for the MT part). The superheat is controlled to avoid flooding of compressors.
- Suction pressure at the LT compressors pack (consisting of a inverter driven 2JME-3K and a 2GME-4K from Bitzer) is controlled by use of the LT compressor pack.
- Suction pressure at the MT compressor pack (consisting of two inverter driven 4MTC-10K and one 4JTC-15K from Bitzer) is controlled in the same manner.
- Temperature of the coolant from the LT compressor pack is controlled by adjusting the flow on the secondary side of the heat exchanger (called desuper-

heater). This temperature is controlled to help reducing the superheat at the suction of the MT compressor pack.

Note that the desuperheater and display cases are not considered in this work. Additionally, there are several controllers on the secondary side which are not of interest, they are mainly used for simulating the various loads on the refrigeration system.

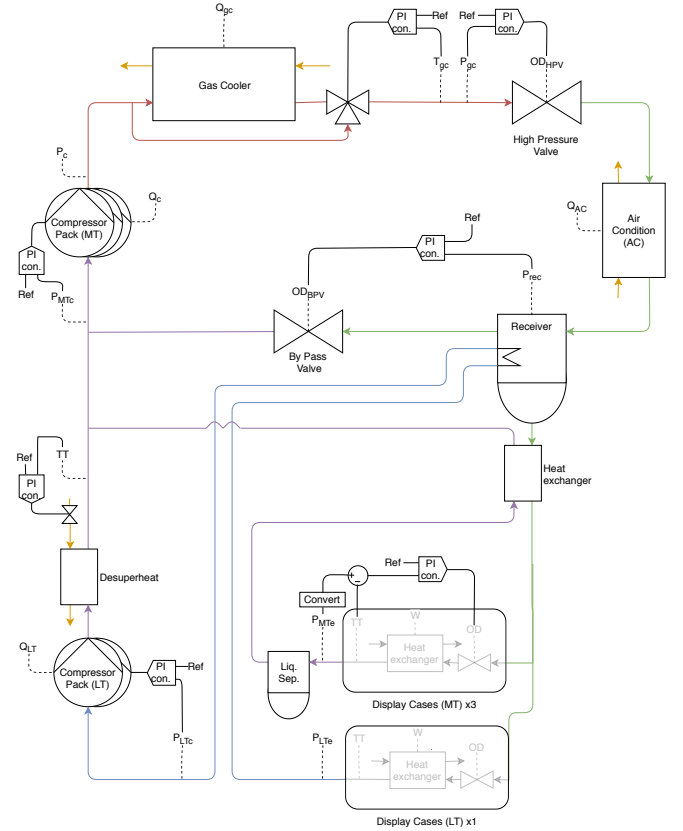


Fig. 1. Illustration of the CO<sub>2</sub> refrigeration system with the selected configuration.

The system is controlled from a local PC where it is possible to manually change system configurations (i.e. activate controller, select controller step point, set system to booster setting, etc.).

### III. SUBSPACE IDENTIFICATION

Subspace identification is utilized as there exist robust algorithms for implementation and it does not suffer from the drawback mentioned in the prior. The purpose of subspace identification is to obtain linear state space models by utilizing experimental input/output (I/O) data. In this paper we consider a discrete-time LTI system described by:

$$x(t+1) = Ax(t) + Bu(t) + Ke(t) \quad (1)$$

$$y(t) = Cx(t) + Du(t) + e(t) \quad (2)$$

where  $x \in \mathbb{R}^n$  is the state vector,  $u \in \mathbb{R}^m$  the input vector,  $y \in \mathbb{R}^l$  the output vector,  $e \in \mathbb{R}^l$  the (innovation) white noise vector and  $A \in \mathbb{R}^{n \times n}$ ,  $B \in \mathbb{R}^{n \times m}$ ,  $C \in \mathbb{R}^{l \times n}$ ,  $D \in \mathbb{R}^{l \times m}$  are constant matrices. The problem is now to identify the

dimension  $n$  and the system matrices (A,B,C,D,K) based on the given I/O data. It should be mentioned that there are several subspace identification methods to solve this problem. The difference between them are how the design variables are selected, it is not yet known how to select them optimally [5], [13], [7]. To solve this problem the following assumptions are needed:

- 1 The number of measurements are sufficiently large (i.e.  $N \rightarrow \infty$ ).
- 2 The inputs ( $u(t)$ ) are persistently excited.
- 3 The inputs are uncorrelated with the noise  $e(t)$  (open-loop data).

The following input-output equations are derived by recursive substitution of equations (1) and (2).

$$Y_f = \Gamma X_f + H^d U_f + H^s E_f \quad (3)$$

$$Y_p = \Gamma X_p + H^d U_p + H^s E_p \quad (4)$$

where  $\Gamma \in \mathbb{R}^{im \times n}$  is the extended observability matrix,  $H^d \in \mathbb{R}^{im \times il}$ ,  $H^s \in \mathbb{R}^{im \times im}$  are lower triangular Toeplitz matrices with the superscripts  $d, s$  denoting deterministic and stochastic inputs ( $u, e$ ) respectively.  $Y_f, Y_p, U_f, U_p$  are block Hankel matrices and are built with the I/O data obtained from the system, i.e:

$$U_p = \begin{bmatrix} u(0) & u(1) & \cdots & u(N-1) \\ u(1) & u(2) & \cdots & u(N) \\ \vdots & \vdots & \ddots & \vdots \\ u(i-1) & u(i) & \cdots & u(i+N-2) \end{bmatrix}$$

$$U_f = \begin{bmatrix} u(i) & u(i+1) & \cdots & u(i+N-1) \\ u(i+1) & u(i+2) & \cdots & u(i+N) \\ \vdots & \vdots & \ddots & \vdots \\ u(2i-1) & u(2i) & \cdots & u(2i+N-2) \end{bmatrix}$$

where  $i > n$ ,  $N$  is sufficiently large and the input data utilized for the block Hankel matrices is partitioned into future ( $f$ ) and past ( $p$ ) measurements.  $Y_f$  and  $Y_p$  are obtained similarly. Note that for simplicity the number of row blocks in the future Hankel matrices are here shown to be the same as the past although they could be chosen different from one another. The future and past state sequences are:

$$X_f = [x(i+1) \quad x(i+2) \quad \cdots \quad x(i+N)]$$

$$X_p = [x(1) \quad x(2) \quad \cdots \quad x(N)]$$

The equations (4) and (3) can be reformulated as:

$$Y = \Gamma X + H^d U + H^s E$$

where  $Y = [Y_f \quad Y_p]^T$ ,  $X = [X_f \quad X_p]^T$  and  $U = [U_f \quad U_p]^T$ . The contribution of  $U$ -term can be removed by utilizing orthogonal projection and the noise term ( $E$ ) is removed by correlating it away with a suitable vector, often chosen to consist of the past inputs and past outputs. The observability matrix multiplied with the states ( $X$ ) can then be found as [7]:

$$\Gamma X \approx \frac{1}{N} Y \Pi_{U^T}^\perp W_p^T = \xi$$

where  $W_p = [U_p \quad Y_p]^T$  and  $\Pi_{U^T}^\perp = I - U^T(UU^T)^{-1}U$ . The extended observability matrix is obtained by first utilizing the SVD (Singular Value Decomposition) of  $W_1 \xi W_2$ :

$$W_1 \xi W_2 = [U_1 \quad U_2] \begin{bmatrix} \Sigma_1 & 0 \\ 0 & \Sigma_2 \end{bmatrix} \begin{bmatrix} V_1 \\ V_2 \end{bmatrix}$$

with  $\Sigma_1 \in \mathbb{R}^{n \times n}$  and  $\Sigma_2 \approx 0$ . Then the extended observability matrix is found as:

$$\Gamma = W_1^{-1} U_1 \Sigma_1^{1/2} T$$

where  $W_1$  and  $W_2$  are weights to be selected, and  $T$  is an arbitrary matrix. From  $\Gamma$  the state space matrices  $A$  and  $C$  can be identified. Where  $A$  is obtained solving a linear equation and  $C$  is directly obtained from  $\Gamma$  as (remark, Matlab<sup>®</sup> notation is used):

$$A = \Gamma(1 : (i-1) \cdot l, 1 : n)^\dagger \cdot \Gamma(l+1 : i \cdot l, 1 : n)$$

$$C = \Gamma(1 : l, 1 : n)$$

Then  $B$  and  $D$  are derived by solving the linear regression:

$$\arg \min_{B, D} \frac{1}{N} \sum_{t=1}^N \|y(t) - C(qI - A)^{-1} B u(t) - D u(t)\|^2$$

This equation is often an overdetermined problem. Lastly, the stochastic part ( $K$ ) is obtained by solving:

$$K e(t) = \hat{x}(t+1) - A x(t) - B u(t)$$

$$e(t) = y(t) - C \hat{x}(t) - D u(t)$$

with the estimated states defined as  $\hat{X} = [\hat{x}(1) \quad \hat{x}(2) \quad \cdots \quad \hat{x}(N)]^T = T^{-1} \Sigma_1^{1/2} V_1^T W_2$  it is straightforward to estimate  $K$  as well as the covariance matrix for the noise ( $e(t)$ ) [7]. The parameters to be chosen are  $T, W_1, W_2, i$  and  $n$ .  $T$  is typically selected to be  $I$  (the identity matrix),  $\Sigma_1$  or  $\Sigma_1^{1/2}$ . Some of the present algorithm use:

- N4SID.  $W_1 = I, W_2 = (\frac{1}{N} W_p Y_f \Pi_{U^T}^\perp W_p^T)^{-1} W_p$ .
- MOESP.  $W_1 = I$  and  $W_2 = (\frac{1}{N} W_p Y_f \Pi_{U^T}^\perp W_p^T)^{-1} W_p \Pi_{U^T}^\perp$ .

Refrigeration systems are open-loop unstable, thus for the assumptions to hold an *Direct Approach* [5] is applied, meaning that the existence of the feedback loop is ignored and open-loop identification is directly applied.

#### IV. DEFINING INPUTS AND OUTPUTS

Generally, adding more (relevant) inputs improves the fit, while adding more outputs have the opposite effect [7]. To achieve accurate estimation, we take the above-mentioned observation into consideration and split the refrigeration system into the following four sub-models:

- Gas cooler - Describes the pressure and temperature before the HPV.
- Receiver - Describes the pressure in the receiver.
- MT compressors - Describes the suction pressure of the MT compressor pack.
- LT compressors - Describes the suction pressure of the LT compressor pack.

The energy and mass balance are utilized to identify the variables that each sub-model is dependent on.

### A. Receiver sub-model

The mass balance for the receiver sub-model is based on the mass flow ( $m$ ) through the HPV, the BPV, MT and LT evaporators:

$$\begin{aligned} \frac{dM_{rec}}{dt} &= m_{HPV} - m_{BPV} - m_{MTe} - m_{LT_e} \\ &= f(OD_{HPV})\sqrt{2\rho_{gc}(P_{gc} - P_{rec})} \\ &\quad - f(OD_{BPV})\sqrt{2\rho_{MTc}(P_{rec} - P_{MTc})} \\ &\quad - \sum_{i=1}^3 f(OD_{MT(i)})\sqrt{2\rho_{MTe}(P_{rec} - P_{MTe})} \\ &\quad - f(OD_{LT})\sqrt{2\rho_{LT_e}(P_{rec} - P_{LT_e})} \end{aligned}$$

where  $f(OD)$  includes the valve characteristics and  $\rho$  is density. By linearizing the above mass balance, the pressure in the receiver ( $P_{rec}$ ) can be isolated, this linearization is not shown here due to its size. A linearized version of a non-linear function will be a linear combination,  $g(\dots)$ , of the variables plus a constant,  $\bar{C}$ :

$$\begin{aligned} P_{rec} &= g(OD_{HPV}, OD_{BPV}, OD_{MT1}, OD_{MT2}, OD_{MT3}, \\ &\quad OD_{LT}, \rho_{gc}, \rho_{HPV}, \rho_{BPV}, \rho_{MTe}, \rho_{LT_e}, P_{gc}, \\ &\quad P_{MTc}, P_{MTe}, P_{LT_e}, \frac{dM_{rev}}{dt}) + \bar{C} \end{aligned}$$

The pressures ( $P_{gc}$ ,  $P_{MTc}$ ,  $P_{MTe}$ ,  $P_{LT_e}$ ) are controlled, thus it is reasonable to assume that the densities ( $\rho_{gc}$ ,  $\rho_{HPV}$ ,  $\rho_{BPV}$ ,  $\rho_{MTe}$ ,  $\rho_{LT_e}$ ) are constant. The mass flow to the evaporators ( $m_{LT_e}$ ,  $m_{MTe}$ ) are assumed negligible for simplicity reasons. With these assumptions the pressure in the receiver can be described as:

$$P_{rec} = g(OD_{HPV}, OD_{BPV}, P_{gc}, P_{MTc}) + \bar{C} \quad (5)$$

Observe the change in mass in the receiver,  $\frac{dM_{rec}}{dt} = V_{rec} \frac{d\rho_{rec}}{dt} = (V_{rec} \frac{d\rho_{rec}}{dP_{rec}}) \frac{dP_{rec}}{dt}$ , is a time constant which the subspace identification method is estimating and is therefore not included in Eq. 5. Lastly, the energy transferred to the AC system ( $Q_{AC}$ ) is included as it has a correlation to  $m_{HPV}$ . The variables, used for the receiver sub-model, are:

Inputs:	$OD_{HPV}$	$OD_{BPV}$	$P_{gc}$	$P_{MTc}$	$Q_{AC}$
---------	------------	------------	----------	-----------	----------

### B. MT and LT sub-models

The purpose of these two sub-models is to describe the pressure before the MT compressor pack ( $P_{MTc}$ ) and LT compressor pack ( $P_{LTc}$ ). The mass balance is not used for these two sub-models as there is a pressure sensor located at the outlet of the MT and LT evaporators ( $P_{MTe}$ ,  $P_{LT_e}$ ). The pressure loss ( $P_{loss}$ ) across a horizontal pipe (between  $P_1$  and  $P_2$ ) is:

$$P_{loss} = P_2 - P_1$$

It is known that the pressure loss depends on pipe and fluid characteristics (constants) as well as the mass flow and whether it is turbulent or laminar flow (variables). Thus, the effect of turbulent flow and mass flow is assumed to be negligible. Hence, the respective pressure measurement at the outlet of the evaporators ( $P_{MTe}$  and  $P_{LT_e}$ ) are sufficient for obtaining a model of  $P_{MTc}$  and  $P_{LTc}$ .

### C. Gas cooler sub-model

The gas cooler sub-model covers modeling of the pressure and temperature before the HPV. It should be mentioned that the three way valve opening degree is not available and is thus not considered as an input for the sub-model. The energy balance is:

$$\begin{aligned} \frac{dM_{gc}h(P_{gc}, T_{gc})}{dt} &= m_c h(P_c, T_c) \\ &\quad - m_{HPV} h(P_{rec}, T_{rec}) - Q_{AC} - Q_{gc} \end{aligned}$$

Using the same principles as for the receiver sub-model the following inputs for the gas cooler sub-model are selected:

Inputs:	$OD_{HPV}$	$\omega_c$	$Q_{gc}$	$Q_{AC}$
	$T_{rec}$	$T_c$	$P_{rec}$	$P_c$

where the mass flow from the MT compressor pack ( $m_c$ ) is described using the speed of the compressor ( $\omega_c$ ). The compressor speed is utilized as the compressors are a positive displacement type.

## V. VALIDATION OF THE DATA-DRIVEN MODEL

Experimental data is obtained from the test setup at NTNU, Trondheim. The experimental data set utilized for training and validation is obtained with active controllers except for the control of the temperature before the HPV. The references are selected as stated below:

Ref.:	$P_{rec}$	$P_{gc}$	$T_{gc}$	$P_{LT}$	$P_{MT}$
Value:	38 [bar]	-	-	14.3 [bar]	28 [bar]

All pressure units are stated in absolute pressure throughout the paper. The reference for the pressure before the HPV is controlled for optimization purposes. The references for the superheat on the three evaporators are set to 8 C. Lastly, the three loads (AC, MT and LT) are varied as shown in Fig. 2. The data-driven model (consisting of the four sub-models) is trained on the first half (0 to 140 minutes) of the data set and validated with the entire data set. It should be noted that the three way valve at the gas cooler is set at a fixed position. The data-driven model derived is a fifth order discrete-time LTI state space model with a sample time of five seconds with poles located as stated below:

GC	Rec.	MT comp.	LT comp.
$0.9213 \pm 0.2332i$	0.9578	0.6016	0.5740

The validation of the pressure ( $P_{gc}$ ) and temperature ( $T_{gc}$ ) before the HPV is shown in Fig. 3. The data-driven model shows a good fit for the pressure, this is caused by the pressure measurement at the MT compressor discharge which

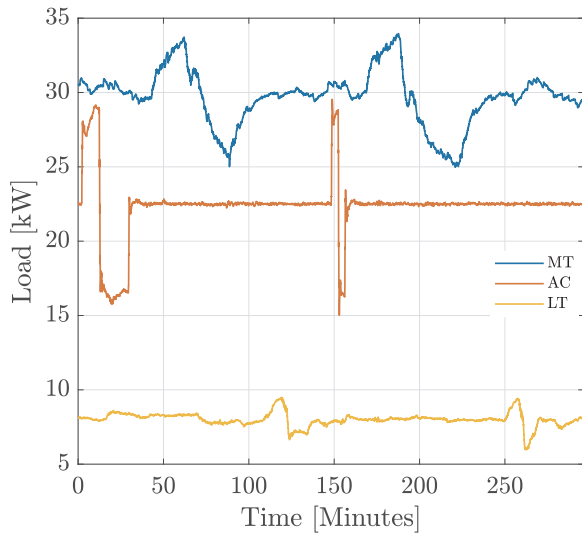


Fig. 2. Illustration of the AC, MT and LT loads in the data set.

is a pressure measurement upstream, thus a pressure drop dependent on gas cooler and piping of the CO<sub>2</sub> refrigeration system. The temperature also shows a good fit, which is in part caused by the strong correlation between the pressure ( $P_{gc}$ ) and the temperature ( $T_{gc}$ ). The remaining outputs are

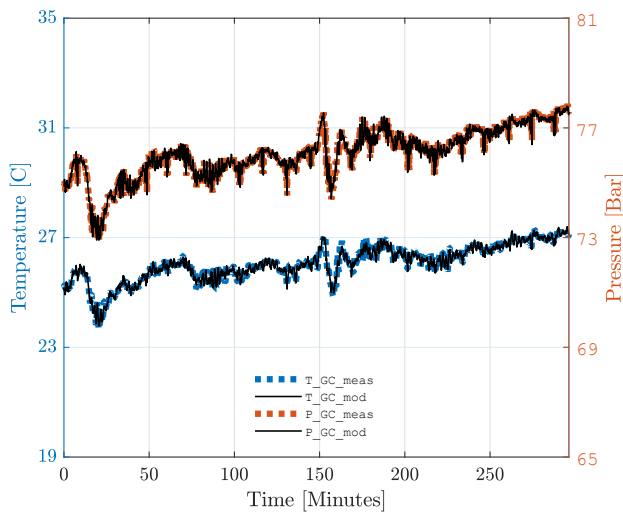


Fig. 3. Illustration of pressure and temperature before the high pressure valve, both measured (red and blue) and outputs from the data-driven model (black).

shown in Fig. 4 which are receiver pressure ( $P_{rec}$ ), suction pressure at MT compressor ( $P_{MTC}$ ) and suction pressure at LT compressor ( $P_{LTC}$ ). MT and LT pressures fit very well due to the pressure measurements at the outlet of the respective display cases. The receiver pressure and MT suction pressure exhibit the same behavior. Hence, the MT suction pressure could be the cause for the good fit for the receiver pressure.

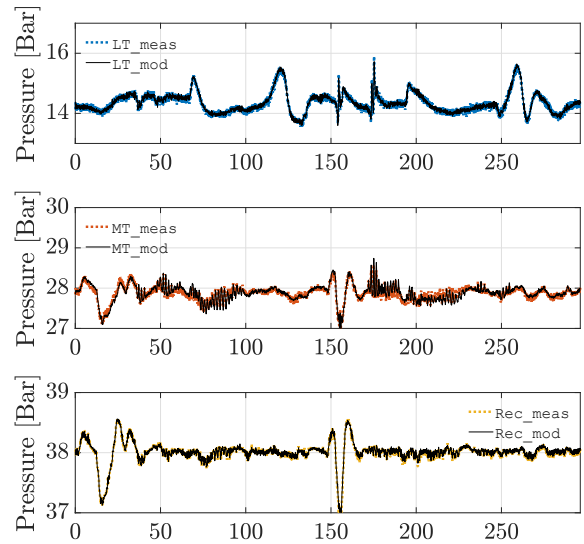


Fig. 4. Illustration of receiver, MT and LT compressor suction pressures. The blue ( $P_{LTC}$ ), red ( $P_{MTC}$ ) and yellow ( $P_{rec}$ ) represent the measure values and the black lines represent outputs from the data-driven model.

#### A. Change in operating condition

Several data sets have been obtained, some of them would be beneficial to include here for validation purposes. However, with the limited space only a few are shown in the following.

The pressures at MT and LT compressor suction are robust to changes in operating conditions. However, variations in operating condition (e.i. mass flow which is caused by change in load for the respective display case) can cause a small deviation. The effect of a large changing in load (hence mass flow) can be seen in Fig 5 where the MT load is changed from maximum (60 kW) to nominal (30 kW). Additionally, in Fig 5 a fit using least squares (LS) is also included, since the dynamic of a pressure drop across a relatively short pipe is fast (hence, it would be reasonable to assume the dynamics for MT and LT compressor sub-models to be negligible). Note that the least squares fit (red line in Fig. 5) and the output from the data-driven model (black line in Fig. 5) are very close to one another and are therefore hard to distinguish. The receiver pressure has the best performance of all the sub-models, even though the CO<sub>2</sub> system includes an AC system. As previously mentioned, the receiver pressure exhibits the same behavior as the pressure at the MT compressor suction. Hence, it could be that a LS could obtain the same performance as the data-driven model. A least squares model is therefore compared with the data-driven model on the same data set as shown in Fig. 5, the result is shown in Fig. 6. The gas cooler is subject to change in ambient temperature along with the effect of the three way valve. Unfortunately, there are no data set available to validate these effects and is therefore subject to future work. The data set in Fig. 5, 6 have the three way valve set to

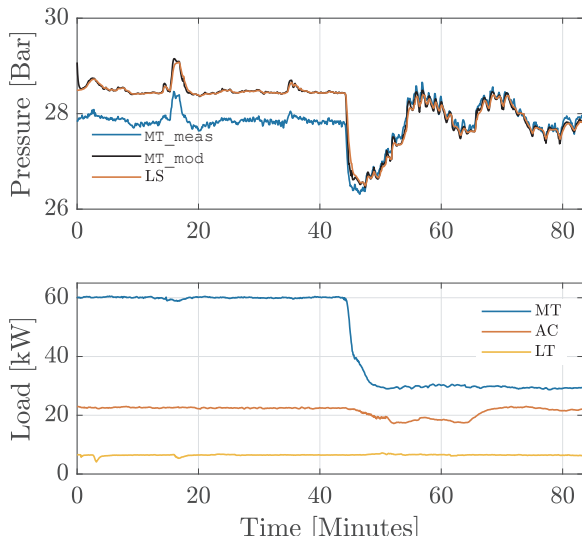


Fig. 5. Lower figure shows the load for the data set. Upper figure shows the suction pressure at MT compressor pack, where blue is measured value, black is data-driven model output, red is obtained using least squares.

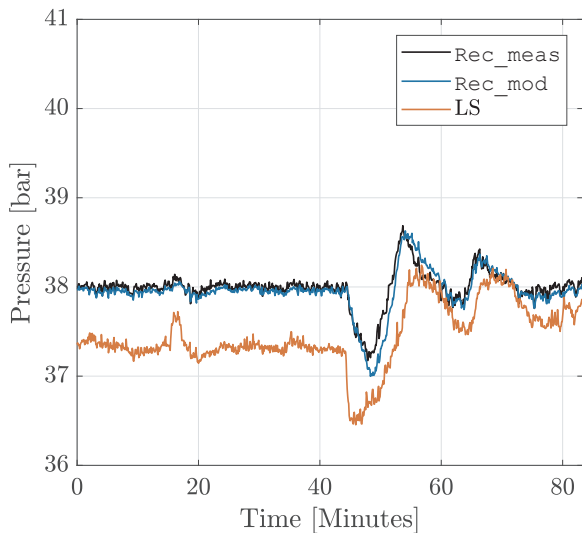


Fig. 6. Illustration of receiver pressure, blue is measured value, black is data-driven model output, red is obtained using least squares method.

a different position than the data set used for training of the data-driven model. Thus, the results with that data set is therefore not shown.

## VI. CONCLUSION

In this paper subspace identification is utilized to derive a data-driven model (consisting of four sub-models, three SISO and one MIMO) which describes the controlled variables i.e. temperature and pressure before the HPV, suction pressures at MT and LT compressor packs and receiver pressure in an industrial CO<sub>2</sub> refrigeration system. The data-driven model shows a good fit as it exploits the strong correlation between the measured variables and the respective output in each sub-model. The strong correlation between the measured

variables and respective outputs are normally not utilized due to the dependency of the refrigeration system. However, this paper shows that data-driven methods (in particular the subspace identification) can conveniently be employed to develop sufficiently accurate models of different subsystems in an industrial refrigeration plant. The perspective would be to utilize these models for the purpose of developing new algorithms for fault diagnosis and fault tolerant control as well as overall system optimization.

## REFERENCES

- [1] K. Vinther, "Data-Driven Control of Refrigeration Systems," Ph.D. dissertation, Aalborg University, 2014.
- [2] S. E. Shafiei, "Control Methods for Energy Management of Refrigeration Systems," Ph.D. dissertation, Aalborg University, 2015.
- [3] B. L. Ho and R. E. Kalman, "Editorial: Effective construction of linear state-variable models from input/output functions," *Automatisierungstechnik*, pp. 545–548, jan 1966.
- [4] K.-J. Åström and B. Torsten, "Numerical Identification of Linear Dynamic Systems from Normal Operating Records," *IFAC Proceedings Volumes*, vol. 2, no. 2, pp. 96–111, sep 1965.
- [5] T. Katayama, *Subspace Methods for System Identification*. Springer, 2005.
- [6] P. Van Overschee and B. De Moor, "Closed loop subspace system identification," *Proceedings of the 36th Conference on Decision & Control*, vol. 2, no. December 1997, pp. 1848–1853, 1997.
- [7] L. Ljung, *System Identification: Theory for the User*, 2nd ed. Prentice-Hall, 1999.
- [8] S. X. Ding, *Data-driven Design of Fault Diagnosis and Fault-tolerant Control Systems*, M. A. Grimble, Michael J.; Johnson, Ed. Springer, 2014.
- [9] S. Yin, S. X. Ding, X. Xie, and H. Luo, "A Review on Basic Data-Driven Approaches for Industrial Process Monitoring," *IEEE Transactions on Industrial Electronics*, vol. 61, no. 11, pp. 6418–6428, nov 2014.
- [10] Z. Chen, S. X. Ding, H. Luo, and K. Zhang, "An alternative data-driven fault detection scheme for dynamic processes with deterministic disturbances," *Journal of the Franklin Institute*, vol. 354, no. 1, pp. 556–570, 2017.
- [11] P. Gullo, K. M. Tsamos, A. Hafner, K. Banasiak, Y. T. Ge, and S. A. Tassou, "Crossing CO<sub>2</sub> equator with the aid of multi-ejector concept: A comprehensive energy and environmental comparative study," *Energy*, vol. 164, no. c, pp. 236–263, 2018.
- [12] Á. A. Pardiñas, A. Hafner, and K. Banasiak, "Integrated R744 ejector supported parallel compression racks for supermarkets. Experimental results," *13th IIR Gustav Lorentzen Conference on Natural Refrigerants: Natural Refrigerant Solutions for Warm Climate Countries*, 2018.
- [13] P. Van Overschee and B. De Moor, *Subspace Identification For Linear Systems*. Kluwer Academic, 1996.